ACS Sustainable Chemistry & Engineering

pubs.acs.org/journal/ascecg

Research Article

Horizons in Coupling of Sulfur-Bearing Silanes to Hydrothermally Treated Lignin toward Sustainable Development

Priyanka Sekar,[⊥] Ricardo P. Martinho,[⊥] Auke G. Talma, Hubert Gojzewski, Alexander Stücker, Bernhard Schwaiger, Jacob Podschun,* and Anke Blume*

Cite This: *ACS Sustainable Chem. Eng.* 2023, 11, 16882−16892

Read Online

ACCESS | Metrics & More | Article Recommendations | Supporting Information

ABSTRACT: The development of hydrothermally treated (HTT) lignin as a promising reinforcing filler for elastomers is challenged by the use of different sulfur-bearing silane coupling agents. Though the application of certain sulfur silane-modified HTT lignin, in particular bis(3-triethoxysilylpropyl)tetrasulfide, improves the in-rubber properties relative to the unmodified and other sulfur silane-modified ones, it results in the formation of distinctive spongelike filler textures within the rubber matrix, as observed by atomic force microscopy. It is of prime importance to understand the reason behind this formation of emerging filler cluster units and the less reinforcing efficiency of other sulfur silane-modified ones. This demanded the elucidation of the coupling reaction of hydrothermally treated lignin and sulfur silane modifiers as it can widen the application window for hydrothermally treated lignin in rubber technology and facilitate the use of these renewable materials. To gain insight into this phenomenon, HTT lignin and their model compounds were subjected to modifications using coupling agents bearing the specific silane functionalities, alkoxy and thiol. By detailed nuclear magnetic resonance investigations, it is shown that the underlying principle of coupling occurs between the thiols of silane and lignin. This systematic study also exemplifies that the ethoxy and/or the silanol groups of silane are unreactive toward the lignin surface and are only capable of self-condensation. In summary, a different coupling phenomenon is observed for hydrothermally treated lignin and sulfur silane, explaining both the cluster formation and the obtained reinforcing properties.

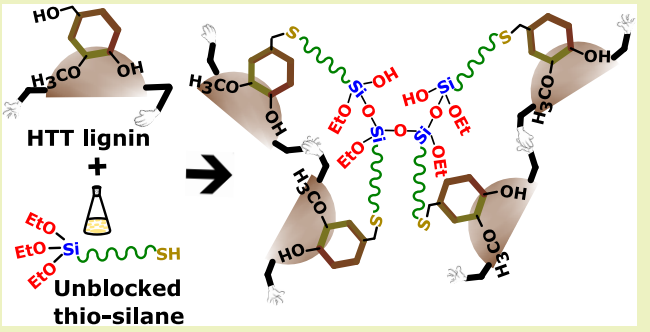

KEYWORDS: *HTT lignin/silane coupling, different coupling, spongelike lignin structures, mercaptopropyltriethoxysilane/HTT lignin, vanillyl alcohol/mercaptopropyltriethoxysilane, lignin model/silane, vanillyl alcohol/1-hexanethiol*

1. INTRODUCTION

In recent years, the application of biobased renewable materials as a potential reinforcing filler has gained interest for the development of sustainable rubber compounds. In this endeavor, lignin recovered from side-streams of, e.g., paper production is being explored extensively due to its abundancy, high carbon content, nonedible nature, and renewability, combined with economic and sustainability benefits.[1−3] Although numerous publications highlight the potential of different technical lignins like Kraft, lignosulfonate, organosolv lignin, etc., as fillers,[4−12] the effective utilization of them in high-end rubber applications, e.g., tires, still poses challenges. This is mainly due to its low thermal stability, structural heterogeneity, varied interunit linkages, functionalities, and the diverse specific properties obtained due to differences in the biomass feedstock and the employed biorefinery processes.[13−16] The sustainable and feasible exploitation of lignin as a filler demands a consistent product with predictable reinforcing properties. One of the promising strategies to produce more homogeneous lignin of a higher purity can be obtained via hydrothermal treatment (HTT). This technique produces thermally stable solid carbonaceous lignin materials with adjustable particle morphology and properties.[17−20] It also yields different lignins with varying particle size distributions and surface functionalities depending on the process conditions.[16,18,19] The presence of still available polar functional groups offers a hydrophilic nature to the HTT lignin and at the same time makes it versatile for surface modification. This is highly beneficial as it can improve the compatibility when incorporated in nonpolar elastomers, as reported in prior arts.[10−12] Especially, surface modifiers, like organosilane coupling agents ($R'Si(OR)_3$), are widely used in the rubber industry to overcome the polarity differences between hydrophilic silica fillers and hydrophobic rubbers.[21−25] These molecules function by anchoring the silica filler and rubber with its two different reactive moieties: (i) the alkoxy

Received: June 13, 2023
Revised: November 5, 2023
Accepted: November 6, 2023
Published: November 21, 2023

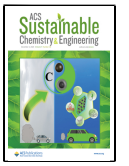

group that can attach to the filler surface bearing silanol groups[26,27] and (ii) the organo functionality, such as sulfide, mercapto, etc., that can interact with rubber.[24−27] The advantages of having such a filler−polymer coupling is well known from the silica/silane system.[28,29]

Initial work carried out to understand the reinforcing potential of HTT lignin in solution styrene butadiene and butadiene rubber blend (SSBR/BR) with and without bis(3-triethoxysilylpropyl)tetrasulfide (TESPT) highlighted that modified HTT lignin shows a superior in-rubber performance compared to the unmodified one. Furthermore, the morphological investigations conducted using the atomic force microscopy (AFM) technique demonstrated the existence of spongelike HTT lignin filler cluster units of 2−3 μm in size in the rubber matrix of TESPT-modified HTT lignin in contrast to the unmodified one. This type of filler structure formation affects the dispersion and distribution behavior of the HTT lignin filler and thus makes it a semireinforcing filler in comparison to the high-reinforcing carbon black and silica filler.[30] The reason for the formation of this HTT lignin cluster is still unknown, and this is the bottom line to understand from the development perspective as it exacerbates the difficulty in advancing HTT lignin as a reinforcing filler.

Further, a similar investigation carried out using two different organosilane coupling agents, (i) (3-thiopropyl)(di-tridecyl-penta-ethoxylate)monoethoxysilane (Si363), a sterically shielded mercaptosilane, and (ii) 3-octanoylthio-1-propyltriethoxysilane (NXT), a chemically blocked mercaptosilane, highlighted that the NXT-modified HTT lignin compound exhibits inferior in-rubber properties comparable to the TESPT- and unmodified HTT lignin-filled ones.[31] And a recent morphological characterization performed for these rubber samples using AFM showed a distinguished behavior (presented in Figure S1) in comparison to the TESPT-modified one reported in prior art.[30] In addition, the morphology observed in the NXT- modified sample (Figure S1) is akin to the unmodified one. These conducted studies lead to a debate on whether in general the alkoxy groups of silane are capable of reacting with HTT lignin or if other reaction pathways occur for HTT lignin and silane coupling agents. The results obtained from TESPT- and NXT-modified rubber samples indicate that the sulfur/thiol group in silane is exhibiting a pivotal role in the rubber reinforcement behavior of modified HTT lignin unlike the silica/silane system.[31] This necessitated the need to investigate the coupling principle of HTT lignin and silane.

To gain a deeper knowledge of the coupling principle of HTT lignin and the sulfur-bearing silanes, several fundamental modification studies using HTT lignin and its model representatives were performed to have a comprehensive understanding of its reactivity with functionalized silanes. The HTT lignin model substances used in this work, vanillyl alcohol (VA) and guaiacol (G) (Figure 1,i,ii), are simplified guaiacyl-type lignin representative substructures, frequently occurring in lignins,[32] with either phenolic or a combination of phenolic and aliphatic hydroxyl functional groups susceptible to modifications. It is assumed that other secondary aliphatic hydroxyl groups would have a comparable reactivity.[33] Similarly, as the silanes are composed of two different functionalities, to clarify whether the reaction of silane to HTT lignin takes place via the alkoxy/silanol group (as expected) or differently via the thiol moieties, modifiers were chosen accordingly to bear only the former (Figure 1,iii), the latter (Figure 1,iv), and the combination of both functionalities (Figure 1,v). To elucidate

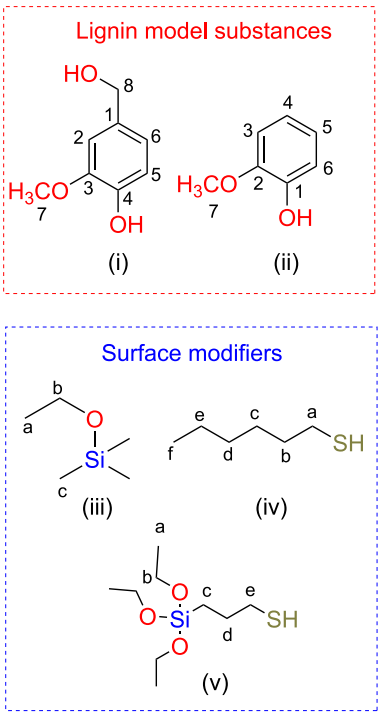

Figure 1. Chemical structures of the HTT lignin model substances: (i) vanillyl alcohol (VA), (ii) guaiacol (G); and the used surface modifiers: (iii) trimethylethoxysilane (TMES), (iv) 1-hexanethiol (HT), and (v) 3-mercaptopropyltriethoxysilane (MPTES).

the coupling reaction, solid-phase modifications were carried out between the selected surface modifiers and HTT lignin as well as between the former and selected HTT lignin model substances. The following characterization tools were used for analyzing the different modified HTT lignins and modified lignin model substances, respectively: (i) standard solid-state analytical techniques, such as thermogravimetric analysis (TGA) and solid-state carbon and silicon nuclear magnetic resonance (^{13}C and ^{29}Si SSNMR), and (ii) one- and two-dimensional liquid ^{1}H-^{13}C NMR. Due to the solubility limitations of HTT lignin, liquid-state characterization techniques were excluded.

The evaluation of the reaction of HTT lignin and its model substances with different surface modifiers in the present study will be useful for the assessment of the surface chemistry and reactivity of HTT lignin and, subsequently, the reinforcing behavior in rubber. Furthermore, it helps to clarify some of the remaining ambiguities in view of the morphological characteristics.

2. EXPERIMENTAL SECTION

2.1. Materials. Commercially available materials were purchased and used as received without further purification or pretreatment, unless otherwise stated. HTT lignin (pH 8.7), with a BET specific surface area of 37 m^2/g, was provided by SunCoal Industries GmbH, Germany. TMES (98%, boiling point or bp 76 °C); HT (95%, bp 154 °C); MPTES (≥80%, bp 215 °C); VA (98%), G (98%); and deuterated dimethyl sulfoxide (DMSO-d_6, 99%) were acquired from Merck KGaA, Germany.

2.2. Modification Procedure. *2.2.1. Direct Reaction of HTT Lignin with Different Surface Modifiers.* All modification variants were performed with the same quantity of solid HTT lignin powder (2 g, 0.64 mmol of phenolic hydroxyl groups) and the liquid modifiers (8.46 mmol) without any solvent. This type of modification protocol was selected and followed in order to replicate the rubber mixing condition.

https://doi.org/10.1021/acssuschemeng.3c03497
ACS Sustainable Chem. Eng. 2023, 11, 16882−16892

An excess amount of modifier (13.5 times) in relation to the available phenolic hydroxyl groups was used in order to improve the wetting of HTT lignin. The described protocol is identical for all of the used modifying agents. HTT lignin and the modifier were added in a 100 mL round-bottom flask equipped with a magnetic stirrer and a reflux condenser. The reaction mixture was refluxed in order to keep all of the low boiling liquids (the surface modifier, reaction products) inside the flask. With this setup, the mixture was heated under constant stirring in an oil bath at 160 ± 5 °C for an hour. After this, the reaction product was extracted in a Soxhlet unit with acetone for 24 h to remove the unreacted and physically adsorbed modifier and afterward placed in a vacuum oven at a temperature of 80 °C for 24 h to remove the solvent.

A physical mixture of MPTES (8.46 mmol) and HTT lignin (2 g) was prepared at room temperature to distinguish the changes caused by physical and chemical interactions. Unlike the modified samples, the extraction protocol was not followed for this sample.

2.2.2. Reaction of Lignin Model Substances with Different Surface Modifiers. Equimolar quantities (3 mmol) of VA or G and TMES were placed in a 5 mL glass ampule and sealed with a rubber septum without any solvent. The filled ampule was immersed into an oil bath at 160 ± 5 °C and the reaction was carried out for 1 h under continuous stirring. After this, the reaction was immediately quenched by placing the ampule in liquid nitrogen. An identical procedure was followed for HT and MPTES. No post-treatment steps were applied. Control experiments with only the lignin model substance (VA) were performed under identical conditions to discard its impact on the analysis of the modified samples. This is denoted as VA-160 in the study.

2.3. Characterization Methods. *2.3.1. Thermogravimetric Analysis (TGA).* To distinguish between the physical and chemical grafting of the different surface modifiers to HTT lignin, the modified samples were subjected to thermal analysis using a TGA 550 analyzer, TA Instruments, USA. Approximately 5−8 mg of the sample was placed in a platinum pan, and all of the samples were first heated isothermally at 30 °C under a nitrogen atmosphere for 10 min, followed by gradient heating from 30 to 600 °C at the rate of 15 °C/min. After incubating at 600 °C for 15 min under nitrogen atmospheric conditions, the samples were further heated from 600 to 900 °C at a heating rate of 15 °C/min under an air atmosphere. Finally, the samples were kept under isothermal conditions at 900 °C for 15 min in an air atmosphere.

2.3.2. Solid-State NMR. ^{13}C SSNMR spectra of different modified HTT lignins and the MPTES-HTT lignin physical mixture were obtained with a Bruker 9.4 T (operating at 400.34 MHz for ^{1}H and at 100.67 MHz for ^{13}C) Avance III HD 400 spectrometer equipped with a 4 mm magic angle spinning (MAS) probe. ^{13}C cross polarization (CP) MAS measurements were conducted at a spinning rate of 14 kHz, with a 90° pulse for ^{1}H of 2.4 μs and a contact time of 2 ms. ^{13}C spectra were internally referenced by the chemical shift of the methoxy peak of lignin (δ = 56.1 ppm) and acquired with 1486 complex points with a spectral width of 295 ppm, with a relaxation delay of 2 s, and acquired with a maximum of 30,000 averages, with sufficient signal-to-noise ratio being ensured.

^{29}Si SSNMR spectra of TMES- and MPTES-modified HTT lignins were obtained with a Bruker 14.1 T (operating at 600.16 MHz for ^{1}H and at 119.23 MHz for ^{29}Si) Avance Neo spectrometer equipped with a 2.5 mm magic angle spinning (MAS) probe. ^{29}Si CP MAS measurements were conducted at a spinning rate of 6 kHz, with a 90° pulse for ^{1}H of 1.94 μs and a contact time of 5 ms. ^{29}Si spectra were externally referenced by the downfield peak of the Q8M8 (trimethylsilyl ester of the double four-ring silicate) reference sample (δ = 12.4 ppm) and acquired with 768 complex points with a spectral width of 381 ppm, a relaxation delay of 15 s, and 17920 averages. All of the SSNMR spectra were zero-filled, apodized with an exponential window function, subjected to phasing, and Fourier-transformed using MestreNova.

2.3.3. Liquid-State NMR. Approximately 10−15 mg of each model reaction mixture was dissolved in 0.5 mL of DMSO-d_6 to be analyzed by NMR. The prepared solutions were characterized by ^{1}H, ^{13}C, ^{1}H-^{13}C heteronuclear single quantum coherence (HSQC), and heteronuclear multiple bond correlation (HMBC) NMR. Experiments were conducted on two different magnets: a Bruker 14.1 T (operating at 600.16 MHz for ^{1}H) Avance NEO spectrometer equipped with a 5 mm BBO solution-state probe and a Bruker 9.4 T (operating at 400.13 MHz for ^{1}H) Avance III spectrometer equipped with a 5 mm BBFO solution-state probe. Both spectrometers were equipped with a 50 G/cm gradient unit on the z axis. All experiments were performed at room temperature. All ^{1}H experiments were measured with a spectral width of 20 ppm, centered at 6.17 ppm, with 16 averages and 32,768 complex points, and a relaxation delay of 2 s. All ^{13}C experiments were measured with a fully decoupled inverse gated sequence, with a spectral width of 262 ppm, centered at 110 ppm, with 1024 averages, acquired with 32,768 complex points, and a relaxation delay of 2 s. All ^{1}H-^{13}C HSQC experiments were fully decoupled and performed with double insensitive nuclei enhancement by polarization transfer (INEPT) tuned to J = 140 Hz, employing an echo/antiecho gradient selection and two phase-cycled scans per t_1 point, with a total of 128 complex t_1 points, a spectral width of 13 ppm in the direct dimension and 210 ppm in the indirect one, and a relaxation delay of 2 s. ^{1}H-^{13}C HMBC experiments were performed using gradient coherence selection optimized for long-range couplings tuned to J = 4 Hz, in order to ensure that ^{4}J and ^{5}J couplings could be observed. Acquisition was performed in the magnitude mode, with 8 phase-cycled averages per t_1 point, with a total of 128 t_1 points, a spectral width of 13 ppm in the direct dimension and 220 ppm in the indirect one, and a relaxation delay of 2 s.

All spectra were zero-filled twice on either one or two dimensions. All spectra were processed with Bruker Topspin, with the 1D spectra being apodized with an exponential window function, while the 2D spectra were apodized with a sine bell (HMBC) and a squared sine bell (HSQC) window function. The ^{1}H and ^{13}C spectra were referenced to the solvent's proton and carbon peaks, respectively.[34] The assignment was performed with the NMRFAM-SPARKY software package.[35] Assignments were performed by resorting to all of the spectra acquired, while cross-referencing these with the Spectral Database for Organic Compounds (SDBS).[36] Specific and cross peaks are displayed in the spectra to elucidate the chemical structures. All peaks that were assigned are displayed in this paper in the Supporting Information (SI).

To investigate if there is a formation of any large solution-state structures, a diffusion-ordered spectroscopy (DOSY) measurement was performed with a stimulated echo and LED sequence, using bipolar gradient pulse pairs.[37] DOSY spectra were obtained with 3 ms gradient length (δ) and with a diffusion time (Δ) of 200 ms, with 32 linearly varying gradient intensities, employing 8 averages. The temperature was kept constant at 25 °C, with an air flow rate of 450 l/h. The obtained ^{1}H spectra are referenced to the DMSO solvent proton peak and the peak assignment is done analogous to the above-described methods. DOSY data were zero-filled, apodized with an exponential window function, subjected to phasing, Fourier-transformed, and subsequently processed with an exponential fitting using MestreNova. The molecular weight of the obtained structures are estimated by using the Stokes−Einstein equation,[38] assuming a spherical shape for the formed structures and the room temperature viscosities and densities for DMSO.[38]

3. RESULTS AND DISCUSSION

3.1. Preliminary Confirmation of the Coupling Reaction between HTT Lignin and the Used Chemicals. TGA measurements were performed for the extracted samples to investigate if the modifiers used are chemically grafted to HTT lignin. The TGA and D-TGA data (depicted in Figure S2a,b) show no significant mass loss for all of the modified HTT lignin below 300 °C. This temperature range is related to the decomposition of low molecular weight residues and the removal of nonchemically bonded compounds. This implies the presence of chemically grafted molecules on the HTT lignin surface or the complete removal of physically interacted chemicals during extraction. In the range between 600 and 900 °C under the air atmosphere, it is observed that MPTES-modified lignin samples (Figure S2a) show a higher residual

https://doi.org/10.1021/acssuschemeng.3c03497
ACS Sustainable Chem. Eng. 2023, 11, 16882−16892

content of 7% compared to the other modified and unmodified HTT lignin samples (4−5%). This signifies that the MPTES-modified HTT lignin sample contains a higher amount of carbonaceous and/or inorganic materials that are stable to the exposed conditions. It could be the result of a higher degree of chemical functionalization of HTT lignin by MPTES and/or the presence of oligomerized MPTES silane on the filler surface formed due to the remaining unreacted ethoxy functionalities. To further discern this, ^{13}C and ^{29}Si NMR studies were carried out.

To confirm the chemical grafting of the modified samples, ^{13}C solid-state NMR was employed to characterize the three modified HTT lignins after extraction, in relation to HTT lignin (Figure 2). Most of the spectral features observed in all of

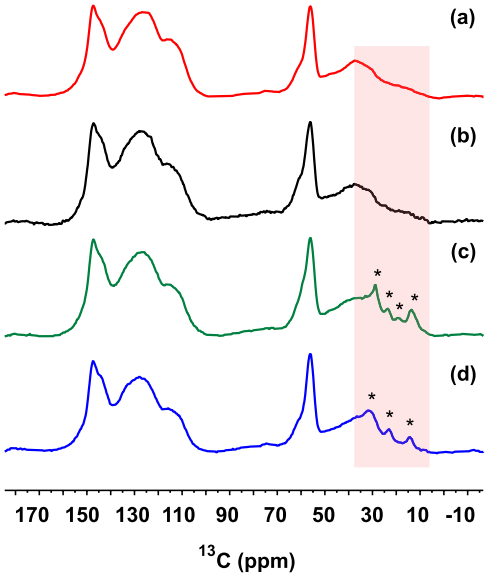

Figure 2. Solid-state ^{13}C NMR spectra of (a) unmodified HTT lignin; and (b) TMES-modified, (c) MPTES-modified, and (d) HT-modified HTT lignin after acetone extraction. The asterix symbol '*' represents the additionally observed peaks. All data were acquired at 9.4 T under MAS conditions at a 14 kHz spinning rate, at room temperature.

these are common to HTT lignin. These signals are qualitatively ascribed to protonated and nonprotonated aromatic carbons ranging between 100 and 160 ppm and to the aliphatic carbons occurring between 0 and 90 ppm; more specifically, the prominent peak at 56 ppm denotes aliphatic O-CH_3.[39,40]

TMES-modified HTT lignin after extraction shows no spectral changes relative to HTT lignin (Figure 2b) and the unextracted one (Figure S3), signifying that the ethoxy group of silane is not capable of coupling to the surface, and this is further confirmed by the absence of ^{29}Si NMR signals (Figure S4a). This ascertains that TMES does not chemically couple to the hydroxyl groups of HTT lignin.

On the contrary, additional peaks (represented by the asterisk '*' symbol) are observed for MPTES- and HT-modified HTT lignin samples (Figure 2c,d) in the region between 10 and 35 ppm. This represents the characteristic aliphatic chain carbons of MPTES and HT (Figure S5 and S6), despite the clear spectral overlap with the signals of HTT lignin in the region between 30 and 40 ppm. This confirms that MPTES and HT are chemically grafted to the HTT lignin surface. The appearance of a new peak around ∼23 ppm in MPTES-modified HTT lignin (Figure S5,iii) and the disappearance of the C-SH peak around ∼24.5 ppm in the HT-modified one (Figure S6,ii) indicate that the thiol functionality is involved in the coupling reaction. Further, though a decrease in the peak intensities of ethoxy carbon a (∼18 ppm) and carbon b (∼58 ppm) is observed, no new peak representing the C−O−C bond arising from the reaction between the ethoxy group of silane and the hydroxyl group of HTT lignin is clearly identified between 50 and 70 ppm. This suggests that this reaction is not preferred and the ethoxy group is involved in other reactions, for e.g., condensation. This is further supported by the absence of the Si−O−C peak and the appearance of new peaks, a representative of self-condensed products in the range between 50 and 70 ppm in the ^{29}Si NMR spectra of MPTES-modified HTT lignin (Figure S4b). Based on the observed ^{29}Si NMR chemical shift value, it can be interpreted that the oligomerized silane is composed of linear (T^2) and three-dimensional Si−O−Si structures (T^3).[41] The chemical structure and the reaction mechanism leading to the formation of oligomeric T^2 and T^3 are well described in the literature[42] and, therefore, the present article will not cover this in detail.

All of these qualitative analyses suggest that the modification of HTT lignin by MPTES is induced only by the thiol moieties and the ethoxy groups of the former are more capable of oligomerizing with another silane molecule.

3.2. Understanding the Reactivity of Functional Groups with HTT Lignin Using Model Studies. Detailed model studies using lignin model substances and different surface modifiers (shown in Figure 1) were performed to further confirm the results of the reaction between HTT lignin and the modifying agents. Since it is known that the lignin model vanillyl alcohol undergoes a condensation and oxidation reaction,[43] an initial study was performed with VA alone (VA-160) to ensure whether this kind of reaction would also occur under the chosen conditions and would interfere with the desired reaction with the surface modifiers. The NMR results of VA-160 (Figure S7) confirm the presence of an oxidation product, vanillin (V), as well as a dimer of VA (DVA), and can be considered side products in the reaction of VA with surface modifiers. The aforementioned reactions occur on the carbon in position 8 of VA (Figure 1A) and thus, based on this ratio, the proportions of V and DVA are quantified as 9 and 13%, respectively, as reported in Table 1. The formation of DVA at 160 °C without any solvent can be expected due to either the generation of a resonance-stabilized benzylic carbocation or a quinone methide (QM) intermediate formed by the reversible elimination of water from a molecule of VA, as described in earlier findings.[43−45] The color

Table 1. Summarized Estimation of the Conversion of HTT Lignin Model Substances (Labeled as LM), G, or VA into Products with Different Surface Modifiers (Labeled as X), TMES, HT, and MPTES[a]

product reactants	remaining LM (%)	oxidized LM (%)	condensed LM (%)	LM_8-X (%)	LM_8-OEt (%)
VA-160	78	9	13	NA	NA
VA+TMES	68	6	13	NI	13
G+TMES	100	NI	NI	NA	NI
VA+HT	NI	7	NI	93	NA
G+HT	100	NI	NI	NA	NA
VA+MPTES	NI	NI	NI	100	NA
G+MPTES	100	NI	NI	NA	NA

[a]LM_8: the reaction occurring at carbon 8 of lignin model substances; OEt: ethoxy residue; NI: not identifiable; NA: not applicable.

https://doi.org/10.1021/acssuschemeng.3c03497
ACS Sustainable Chem. Eng. 2023, 11, 16882−16892

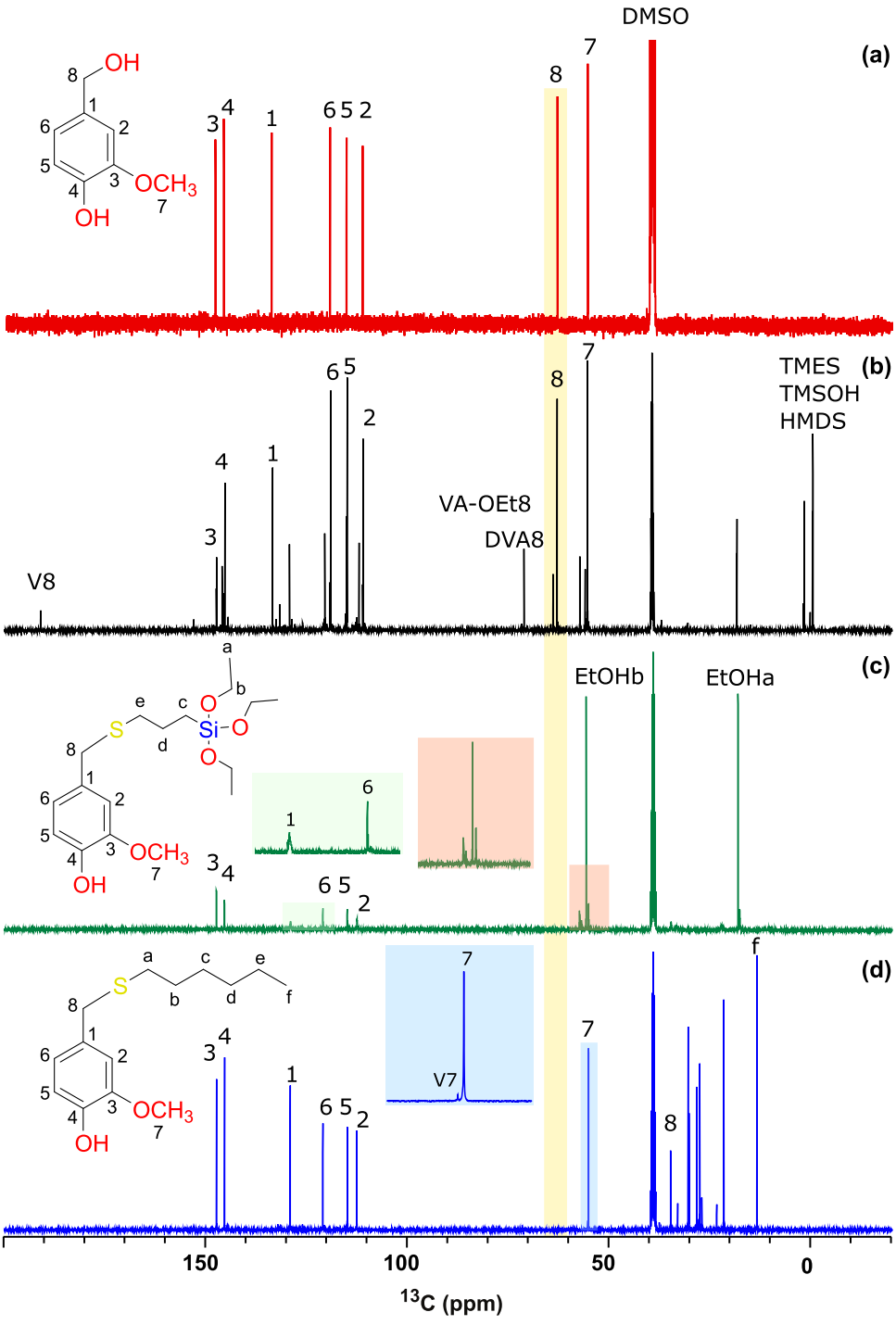

Figure 3. Liquid-state ^{13}C NMR spectra of (a) pure vanillyl alcohol (VA) and the reaction products of vanillyl alcohol (VA) obtained after the reaction at 160 ± 5 °C with (b) TMES, (c) MPTES, and (d) HT. V: vanillin; DVA: dimerized VA; and EtOH (a, b): ethanol. The data were acquired in DMSO-d_6 at room temperature; panel (a) was performed at 14.1 T, whereas panels (b) and (c) were performed at 9.4 T.

change of VA after the reaction (refer to the Supporting Information) suggests the formation of QM, but it could not be identified in the reported spectra (Figure S7). This indicates that the carbocation of VA or the QM intermediates are highly reactive species and it is very difficult to identify and quantify them. Nevertheless, if there is a formation of such intermediates which are electron acceptor species, they can offer a wide range of reactivities, signifying that VA can react with different modifiers.[43,46−49]

For guaiacol, as discussed in Section 2.2.2, the control study was not performed like VA, but from the reactions carried out with different surface modifiers, it can be observed that no significant condensation or oxidation products were identified in the spectra (Figures S8−10). This indicates that under the given reaction conditions, it remains more stable, thus suggesting the need to have an aliphatic hydroxyl group (refer to Figure 1B) for the oxidation or condensation reactions to occur.

Having sorted out the side reactions of lignin model substances at the chosen conditions, the occurrence of the

https://doi.org/10.1021/acssuschemeng.3c03497
ACS Sustainable Chem. Eng. 2023, 11, 16882−16892

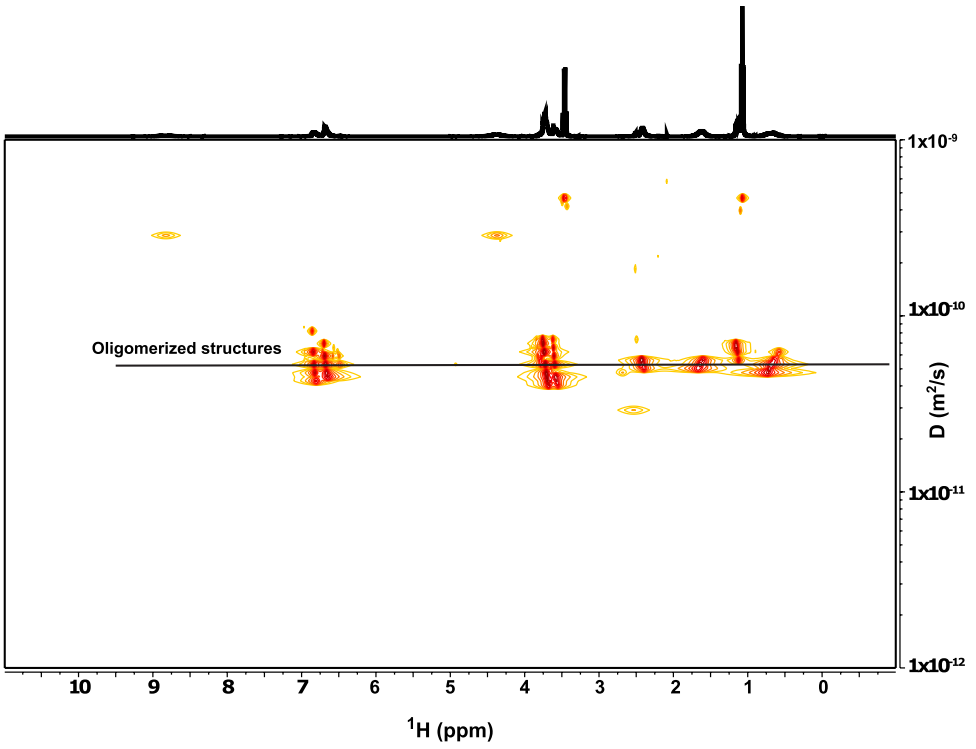

Figure 4. Diffusion-ordered spectroscopy (DOSY) liquid-state NMR spectrum resulting from the reaction of vanillyl alcohol (VA) with MPTES at 160 ± 5 °C. The data were acquired in DMSO-d_6 at 9.4 T at 25 °C.

preferred coupling reaction between the lignin model substances and the surface modifiers was investigated by different 1D and 2D NMRs. The spectra of different reaction mixtures are presented in Figures S8−S13. The summary of all of the relative proportions of the main reaction products as a result of coupling (L-M_8-X) is reported in Table 1. This quantification was performed on clearly distinct and identifiable resonances that were found in the same positions in the molecules. The proportions of the products in the reaction mixtures of vanillyl alcohol and TMES silane (VA+TMES) were determined by the ratios of the carbons in position 8. For the reaction products of vanillyl alcohol and hexanethiol (VA+HT), the proportions were estimated by the ratio of the integrals of the V7 and VA-HT7 ^{13}C peaks. In all other cases in which multiple products were not observed, the final outcome is considered quantitative, for only having the remaining starting material or product.

The study with the lignin model guaiacol did not show any reaction products with any of the modifiers employed in this work, as shown in Figures S8−S10. This confirms that no reaction occurred between the ethoxy/silanol and thiol functionalities and the phenolic hydroxyl or any other aromatic center in the guaiacol molecule.

In contrast, the reactivity of vanillyl alcohol with the modifiers is higher under the used conditions, suggesting that aliphatic hydroxyl group functionalities are vital for the modification. The ^{13}C spectra of the modifications of VA with and without the three modifying agents employed are shown in Figure 3. Condensation and oxidation products could also be observed in the reaction between VA and TMES, as depicted in Figures 3b and S11. The HMBC spectra demonstrated that trimethylsilanol TMSOH could also be identified in the reaction mixture, implying that TMES hydrolyzed under the subjected reaction conditions. TMES hydrolysis was further confirmed by the identification of the product formed as a result of the reaction between ethanol and VA at position 8 (LM_8-OEt, Table 1). This indicates that ethanol, the byproduct of TMES hydrolysis, also reacts with VA and this can be treated as another side reaction. This reaction does not significantly change the amount of other side products formed (dimer or vanillin). Besides the side reactions, no direct coupling products of TMES or TMSOH and VA could be identified. Although the findings of Nathan et al. reported the occurrence of trans-etherification reactions between the primary aliphatic alcohol of VA and ethoxy of silane, under the given conditions, it could not be detected in this study.[50] And thus, it can be concluded that TMES or TMSOH is less reactive toward VA than aliphatic hydroxyl nucleophiles like ethanol.

The reaction with HT, however, resulted in a direct coupling, as can be identified in Figure 3d by the disappearance of the aliphatic hydroxyl carbon in position 8 at ∼62 ppm. A direct coupling between the sulfur atoms of HT and VA could be identified via HMBC (the cross peak between proton 8 and carbon a in Figure S12), which corresponds to a high conversion (∼93%, Table 1). In addition, the findings highlight that the coupling reaction between VA and HT is highly preferred in comparison to the side reactions like oxidation and condensation, unlike TMES.

The reactivity of thiols toward VA was also assessed with the agent MPTES, as demonstrated in Figure 3c, which shows a clearly lower intensity in the spectrum due to broader lines (which could also be observed in the ^{1}H spectrum, as presented in Figures S13 and S16), as well as the absence of the aliphatic hydroxyl carbon in position 8 in the spectrum. This indicated conversion, which could also be observed by an HMBC correlation between proton 8 of the VA moieties (refer to Figure 1A) and the proton at position c of the MPTES one (refer to Figure 1E). No clear leftovers of VA nor its derivatives at these temperatures could be observed, demonstrating a high

https://doi.org/10.1021/acssuschemeng.3c03497
ACS Sustainable Chem. Eng. 2023, 11, 16882−16892

Scheme 1. Coupling Reaction Proposal for HTT lignin-MPTES Silane[a]

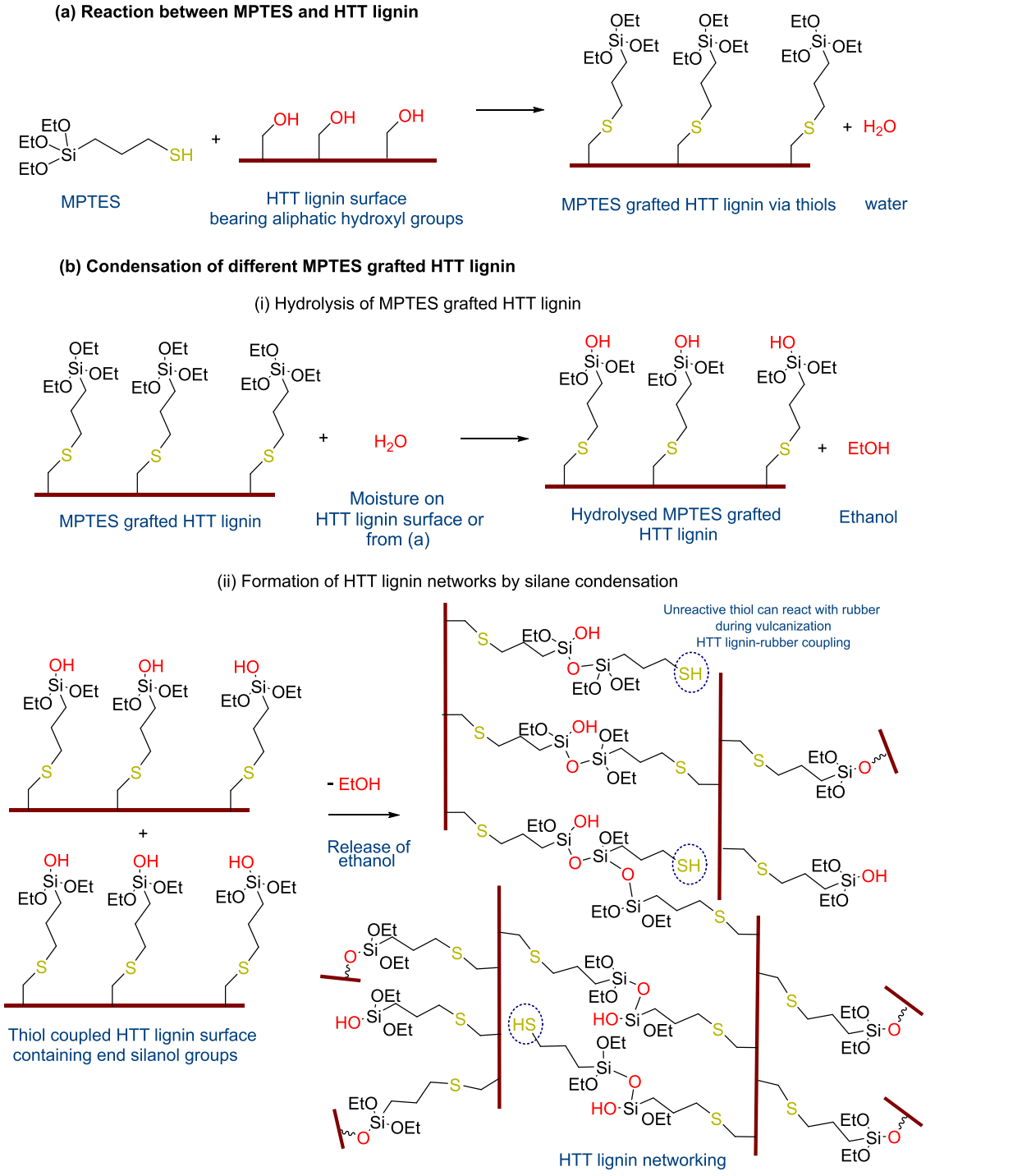

[a](a) Benzylic hydroxyl groups of HTT lignin favoring the addition of MPTES through the possible formation of a quinone methide intermediate (which might be a concerted one); (b) condensation of hydrolyzed silane leading to the formation of HTT lignin filler networks.

selectivity toward the reaction with MPTES, having an approximately quantitative conversion. Furthermore, free ethanol could be observed, which corresponds to ~58% of the total amount in the system (when considering all of the CH_2 protons at position b from MPTES or derivatives, which were integrated). All of these observations indicate a high reactivity of MPTES toward VA. In addition, the observed broader spectral lines suggest the presence of large structural moieties. This was further assessed and confirmed by DOSY NMR (Figure 4), which reports on the diffusivity of molecules in solution. It is possible to observe herein other than a few fast-diffusing molecules, such as ethanol, slow-diffusing structures that incorporate the coupled VA-MPTES structure, with a diffusion coefficient of $\sim 5.8 \pm 1.1 \times 10^{-11}$ m^2/s. The molecular weight of these formed structures is estimated between 11 and 35 kDa, based on the Stokes−Einstein equation.[38] This indicates oligomerized structure(s) established during the reaction of VA and MPTES. Alternatively, the condensation of VA

https://doi.org/10.1021/acssuschemeng.3c03497
ACS Sustainable Chem. Eng. 2023, 11, 16882−16892

molecules via etherification could have occurred; however, the respective structures were not identified in the spectra. Similar effects (large structures) could not be observed for TMES, which can only form dimers (as tentatively identified in Figure S8). It shall also be noted that the DOSY spectrum resulting from the reaction between guaiacol and MPTES (Figure S17) shows only the presence of small molecules, and thus, no oligomerized products could be observed. This is likely due to the absence of sufficient amount of moisture to hydrolyze silane for a subsequent condensation reaction.[51]

Based on the results, it could be observed that no reaction occurred between guaiacol and the modifiers used. On the contrary, the reaction of VA with surface modifiers occurs predominantly at the C8 position. This highlights that the presence of benzylic carbon is a prerequisite for the coupling reaction to occur. In addition, it is recognized that depending on the type of functional group of the surface modifier (−SH, −COH, and −SiOH), the reactivity changes. This indicates that the nature of the functional groups plays a pivotal role in the coupling reaction of VA and surface modifiers. From these findings, the following reaction mechanism can be postulated using the concept of "hard" and "soft" electrophile−nucleophile chemistry (hard and soft acid and base concept).[52,53] Under the used reaction conditions, the phenolic moieties in vanillyl alcohol can be converted to electrophilic p-quinone methide (QM) intermediates by the elimination of water,[33,45,46] as shown in Scheme S1. QM is highly reactive and can undergo resonance stabilization, resulting in a polar zwitterion that is susceptible to nucleophilic attack.[47,49] As QM and the resulting carbocation of the zwitterion are soft electrophiles, the preferred pathway for this reaction depends significantly on the chemical hardness/softness of the used nucleophiles as recognized before.[47] The nucleophilic reactivity toward QM and the resulting carbocations decreases in the following order: C-SH (thiols) > C-OH (hydroxyl from another VA or ethanol) > Si-OH (silanols). Thus, 1-hexanethiol being a soft nucleophile can undergo, on the one hand, addition with QM leading to a thioether formation (6, outlined in Scheme S1).[46−48] On the other hand, due to the comparatively lower polarizability of silanol groups under the given pH value, the reaction of TMES with QM is very slow and unfavorable in the presence of thiols and ethanol (the byproduct of silane hydrolysis). Thus, TMES or MPTES does not react with VA via the ethoxy or silanol functionality, as demonstrated by the results of the VA/TMES and VA/MPTES experiments. Though the proposed reaction scheme (Scheme S1) fits well to the obtained results, the formation of QM was not experimentally confirmed.

3.3. Unraveling the Coupling Principle of HTT Lignin and Sulfur-Bearing Silanes. The ^{13}C NMR, ^{29}Si SSNMR, and all of the liquid NMR data presented in this paper reveal that the thiol functionality plays an important role in the coupling reaction with HTT lignin and its model substances. Similarly, it is also demonstrated that the alkoxy functionalities of silane are less reactive to VA or HTT lignin and are involved in the self-condensation reaction.[42] The occurrence of the coupling and condensation reaction can be evidenced by the ^{13}C NMR (Figures 2 and S6) and ^{29}Si NMR (Figure S4b) spectra of MPTES-modified HTT lignin, respectively. And the ^{13}C NMR (Figure S13) and DOSY NMR spectra (Figure 4) of the model study carried between VA and MPTES further confirmed the C−S coupling and the formation of relatively large structures in the reaction product. This highlights that the surface activity of HTT lignin is different toward silane. This is in contrast to the originally expected mechanism based on the silica/silane interaction where alkoxy groups are predominantly involved in the coupling reactions.[26] Additionally, from the model study, it is apparent that the thiol of silane adds markedly to the aliphatic carbon of VA or HTT lignin through a nucleophilic addition reaction (Scheme S1). Based on the proposed reaction pathway of the lignin model substances and thiol outlined in Scheme S1, the possible coupling reaction between HTT lignin and silane, e.g., MPTES, is exemplified using Scheme 1. This involves the following reactions:

(i) a coupling reaction leading to a covalent thioether bond between HTT lignin and MPTES; a result of the generation of quinone methide or a carbocation electrophile from the available benzylic hydroxyl groups of HTT lignin.

(ii) a condensation reaction between MPTES-grafted HTT lignin and another thiol-modified one. Networks of HTT lignin particles with rubber trapped inside (a spongelike structure) are formed through hydrolysis with the silanol groups of the grafted silane. The hydrolysis of silane can occur either by the moisture available on the surface of HTT lignin (5%) or by the water generated during the coupling reaction of HTT lignin with thiol. These generated silanols can either condense with another silanol group or with an ethoxy silane already attached to the HTT lignin. It is unclear if the hydrolysis step occurs before, after, or in-parallel to the coupling reactions. For simplicity, it is assumed in Scheme 1 that this reaction occurs after the coupling.

It is reported in earlier work that both the coupling and condensation (silane oligomerization of partially hydrolyzed alkoxysilanes) reactions are highly favorable in a basic environment,[46,51,33,54] which means that HTT lignin with a pH of 8.7 promotes both of the above-described reactions. The proposed coupling scheme (Scheme 1) of MPTES can be extended to the other silane containing the HTT lignin-filled rubber compound. For example, for the TESPT/HTT lignin/rubber system, a scheme is depicted (Scheme S2) and this also fits very well with the experimental data (increased uncured Payne effect, Mooney viscosity, improved mechanical properties, etc.) reported in prior art.[30] Similarly, the inferior reinforcing effect of NXT containing the HTT lignin-filled rubber vulcanizate is a result of the lack of a coupling reaction between the filler and silane. This is because the thiol groups of NXT silane are blocked by an octanoyl group, and it is not available for the coupling reaction with HTT lignin. Thus, the subsequent in situ formed spongelike filler structure is absent in this vulcanizate (Figure S1b). Si363 silane can favor both the coupling and condensation reaction in the HTT lignin-filled rubber compound leading to improved reinforcing properties and the spongelike HTT lignin structures (Figure S1a). This suggests that the surface activity of silanes with HTT lignin is the leading factor for the formation of spongelike filler clusters, and both play a vital role in the rubber reinforcement of the HTT lignin filler. It is also to be noted that depending on the silane type, the coupling and condensation reaction varies.

4. CONCLUSIONS

The coupling reaction that can occur between HTT lignin and the organosilane coupling agent is being explored through parallel studies conducted with HTT lignin and its model substances, vanillyl alcohol, and guaiacol, with different surface

https://doi.org/10.1021/acssuschemeng.3c03497
ACS Sustainable Chem. Eng. 2023, 11, 16882−16892

modifiers. A comprehensive NMR investigation carried out on different modified lignin model substances enabled a better understanding of the reaction between HTT lignin and silane. By combining the obtained results of the above-mentioned studies, the following conclusions are derived:

(i) The different surface chemistry of HTT lignin as compared to silica appears to change the reactivity of silane. Thus, the existing reaction mechanism from the silica/silane coupling model cannot be directly transferred to the current system; it requires a completely new mechanistic study.
(ii) Silane is coupled to HTT lignin via the thiol functionality. Under the investigated conditions, the aliphatic hydroxyl groups of HTT lignin are identified as a pivotal moiety for the coupling reaction, whereas, the phenolic hydroxyl ones remain inert. The thiol covalently bonds to the aliphatic carbon of HTT lignin forming a thioether bond (−C−S−).
(iii) The alkoxy groups of silane are mostly involved in the self-condensation reaction rather than participating in the coupling reaction with the functional groups of HTT lignin. The former reaction is mainly responsible for the formation of spongelike lignin clusters in sulfur silane containing the HTT lignin-filled rubber compound.

With this gained knowledge, a different coupling mode for sulfur silane and HTT lignin is proposed, as opposed to the traditional silica/silane ones. This unprecedented mode of reaction provides a straightforward explanation for the formation of spongelike lignin textures in the HTT lignin/TESPT silane-modified rubber compound. It also justifies the previously obtained in-rubber results such as Mooney viscosity, uncured Payne effect, mechanical properties, etc., of different sulfur silanes containing HTT lignin. In particular, the less reinforcing effects of NXT containing the HTT lignin-filled rubber compound are due to the restriction in the coupling reactions. Here, the thiol functionalities are blocked chemically and are unavailable to coupling reactions.

These findings confirm the chemical bonding between HTT lignin and silane coupling agents via the sulfur atom. Also, it can fill the knowledge gap in the modification strategies as well as change the conventional ideology of silanization chemistry for existing lignins.

■ ASSOCIATED CONTENT

Supporting Information

The Supporting Information is available free of charge at https://pubs.acs.org/doi/10.1021/acssuschemeng.3c03497.

It includes the ^{13}C and ^{29}Si NMR spectra of TMES/HTT lignin and MPTES/HTT lignin, the TGA data of all of the modified samples, and the liquid NMR spectra of the reaction product of TMES, MPTES, and HT with vanillyl alcohol and guaiacol (PDF)

■ AUTHOR INFORMATION

Corresponding Authors

Jacob Podschun − *SunCoal Industries GmbH, 14974 Ludwigsfelde, Germany*; Email: podschun@suncoal.com

Anke Blume − *Elastomer Technology and Engineering, Department of Mechanics of Solids, Surfaces and Systems (MS3), Faculty of Engineering Technology, University of Twente, 7500 AE Enschede, The Netherlands*; Email: a.blume@utwente.nl

Authors

Priyanka Sekar − *Elastomer Technology and Engineering, Department of Mechanics of Solids, Surfaces and Systems (MS3), Faculty of Engineering Technology, University of Twente, 7500 AE Enschede, The Netherlands; SunCoal Industries GmbH, 14974 Ludwigsfelde, Germany*; orcid.org/0000-0001-8975-8237

Ricardo P. Martinho − *Department of Molecules and Materials, MESA+ Institute for Nanotechnology, Faculty of Science and Technology, University of Twente, 7500 AE Enschede, The Netherlands*; orcid.org/0000-0003-4223-174X

Auke G. Talma − *Elastomer Technology and Engineering, Department of Mechanics of Solids, Surfaces and Systems (MS3), Faculty of Engineering Technology, University of Twente, 7500 AE Enschede, The Netherlands*

Hubert Gojzewski − *Sustainable Polymer Chemistry, Department of Molecules & Materials, Faculty of Science and Technology, University of Twente, 7522 NB Enschede, The Netherlands*; orcid.org/0000-0001-6325-8293

Alexander Stücker − *SunCoal Industries GmbH, 14974 Ludwigsfelde, Germany*

Bernhard Schwaiger − *SunCoal Industries GmbH, 14974 Ludwigsfelde, Germany*

Complete contact information is available at: https://pubs.acs.org/10.1021/acssuschemeng.3c03497

Author Contributions

$^{\perp}$P.S. and R.P.M contributed equally to this work. The manuscript was written through the contributions of all authors. All authors have given approval to the final version of the manuscript.

Notes

The authors declare no competing financial interest.

■ ACKNOWLEDGMENTS

The authors are indebted to SunCoal Industries GmbH (Germany) for their financial support of the current project as well as the permission to publish this work. A special thanks to Professor Dr. J.W.M. Noordermeer for extending his help and expertise that greatly assisted the research. Dr. R. Anyszka and Dr. F. Grunert are acknowledged for providing insightful feedback related to rubber results. Dr. M. Bacher is kindly acknowledged for supporting the ^{13}C SSNMR analysis.

■ ABBREVIATIONS

CP, cross-polarization; DOSY, diffusion-ordered spectroscopy; G, guaiacol; HMBC, heteronuclear multiple bond correlation; HSQC, heteronuclear single quantum coherence; HT, 1-hexanethiol; HTT, hydrothermal treatment; MAS, magic angle spinning; MPTES, mercaptopropyltriethoxysilane; NXT, 3-octonoylthio-1-propyltriethoxysilane; Si363, 3-thiopropyl(di-tridecyl-penta-ethoxylate)monoethoxysilane; TESPT, bis(3-triethoxysilylpropyl)tetrasulfide; TMES, trimethylethoxysilane; SSNMR, solid-state nuclear magnetic resonance; VA, vanillyl alcohol

■ REFERENCES

(1) Lora, J. H.; Glasser, W. G. Recent Industrial Applications of Lignin: A Sustainable Alternative to Nonrenewable Materials. *J. Polym. Environ.* **2002**, *10* (1), 39−48.

(2) Lawoko, M.; Berglund, L.; Johansson, M. Lignin as a Renewable Substrate for Polymers: From Molecular Understanding and Isolation

to Targeted Applications. *ACS Sustainable Chem. Eng.* **2021**, *9* (16), 5481−5485.
(3) Mariana, M.; Alfatah, T.; H p s, A. K.; Yahya, E. B.; Olaiya, N. G.; Nuryawan, A.; Mistar, E. M.; Abdullah, C. K.; Abdulmadjid, S. N.; Ismail, H. A Current Advancement on the Role of Lignin as Sustainable Reinforcement Material in Biopolymeric Blends. *J. Mater. Res. Technol.* **2021**, *15*, 2287−2316.
(4) Kumaran, M. G.; De, S. K. Utilization of Lignins in Rubber Compounding. *J. Appl. Polym. Sci.* **1978**, *22* (7), 1885−1893.
(5) Keilen, J. J.; Pollak, A. Lignin for Reinforcing Rubber. *Rubber Chem. Technol.* **1947**, *20* (4), 1099−1108.
(6) Setua, D. K.; Shukla, M. K.; Nigam, V.; Singh, H.; Mathur, G. N. Lignin Reinforced Rubber Composites. *Polym. Compos.* **2000**, *21* (6), 988−995.
(7) Košíková, B.; Gregorová, A. Sulfur-Free Lignin as Reinforcing Component of Styrene−Butadiene Rubber. *J. Appl. Polym. Sci.* **2005**, *97* (3), 924−929.
(8) Bahl, K.; Jana, S. C. Surface Modification of Lignosulfonates for Reinforcement of Styrene−Butadiene Rubber Compounds. *J. Appl. Polym. Sci.* **2014**, *131* (7), 1−9.
(9) Barana, D.; Ali, S. D.; Salanti, A.; Orlandi, M.; Castellani, L.; Hanel, T.; Zoia, L. Influence of Lignin Features on Thermal Stability and Mechanical Properties of Natural Rubber Compounds. *ACS Sustainable Chem. Eng.* **2016**, *4* (10), 5258−5267.
(10) Mohamad Aini, N. A.; Othman, N.; Hussin, M. H.; Sahakaro, K.; Hayeemasae, N. Lignin as Alternative Reinforcing Filler in the Rubber Industry: A Review. *Front. Mater.* **2020**, *6*, 329−347.
(11) Hait, S.; De, D.; Ghosh, P.; Chanda, J.; Mukhopadhyay, R.; Dasgupta, S.; Sallat, A.; Al Aiti, M.; Stöckelhuber, K. W.; Wießner, S.; Heinrich, G.; Das, A. Understanding the Coupling Effect between Lignin and Polybutadiene Elastomer. *J. Compos. Sci.* **2021**, *5* (6), 154−169.
(12) Li, M.; Zhu, L.; Xiao, H.; Shen, T.; Tan, Z.; Zhuang, W.; Xi, Y.; Ji, X.; Zhu, C.; Ying, H. Design of a Lignin-Based Versatile Bioreinforcement for High-Performance Natural Rubber Composites. *ACS Sustainable Chem. Eng.* **2022**, *10* (24), 8031−8042.
(13) Rana, R.; N, S.; a Meda, V.; Dalai, A. K.; Kozinski, J. A. A Review of Lignin Chemistry and Its Biorefining Conversion Technologies. *J. Biochem. Eng. Bioprocess. Technol.* **2018**, *1* (2), 1−14.
(14) Boerjan, W.; Ralph, J.; Baucher, M. Lignin Biosynthesis. *Annu. Rev. Plant Biol.* **2003**, *54*, 519−546.
(15) Chakar, F. S.; Ragauskas, A. J. Review of Current and Future Softwood Kraft Lignin Process Chemistry. *Ind. Crops Prod.* **2004**, *20* (2), 131−141.
(16) Crestini, C.; Lange, H.; Sette, M.; Argyropoulos, D. S. On the Structure of Softwood Kraft Lignin. *Green Chem.* **2017**, *19* (17), 4104−4121.
(17) Titirici, M.-M.; Antonietti, M. Chemistry and Materials Options of Sustainable Carbon Materials Made by Hydrothermal Carbonization. *Chem. Soc. Rev.* **2010**, *39* (1), 103−116.
(18) Wikberg, H.; Ohra-aho, T.; Pileidis, F.; Titirici, M.-M. Structural and Morphological Changes in Kraft Lignin during Hydrothermal Carbonization. *ACS Sustainable Chem. Eng.* **2015**, *3* (11), 2737−2745.
(19) Wittmann, T. Method for Obtaining Stabilized Lignin Having a Defined Particle-Size Distribution from a Lignin-Containing Liquid. U.S. Patent US20170247255A1, 2017.
(20) Wittmann, T.; Bergemann, K. Hydrothermal Treatment of Renewable Raw Material. U.S. Patent US20200239697A1, 2020.
(21) Rauline, R. Rubber Compound and Tires Based on Such a Compound. EP0501227A1, Sep 2, 1992. https://patents.google.com/patent/EP0501227A1/en (accessed Aug 17, 2022).
(22) Luginsland, H.-D.; Fröhlich, J.; Wehmeier, A. Influence of Different Silanes on the Reinforcement of Silica-Filled Rubber Compounds. *Rubber Chem. Technol.* **2002**, *75*, 563−579.
(23) Luginsland, H.-D.; Röben, C. The Development of Sulphur-Functional Silanes as Coupling Agents in Silica-Reinforced Rubber Compounds. Their Historical Development over Several Decades. *Int. Polym. Sci. Technol.* **2016**, *43* (4), 1−6.
(24) Reuvekamp, L. A. E. M.; Brinke, J. W.; ten Swaaij, P. J. van.; Noordermeer, J. W. M. Effects of Time and Temperature on the Reaction of TESPT Silane Coupling Agent during Mixing with Silica Filler and Tire Rubber. *Rubber Chem. Technol.* **2002**, *75* (2), 187−198.
(25) Ansarifar, A.; Saeed, F.; Ostad Movahed, S.; Wang, L.; Ansar Yasin, K.; Hameed, S. Using a Sulfur-Bearing Silane to Improve Rubber Formulations for Potential Use in Industrial Rubber Articles. *J. Adhes. Sci. Technol.* **2013**, *27* (4), 371−384.
(26) Goerl, U.; Hunsche, A.; Mueller, A.; Koban, H. G. Investigations into the Silica/Silane Reaction System. *Rubber Chem. Technol.* **1997**, *70* (4), 608−623.
(27) Hunsche, A.; Görl, U.; Müller, A.; Knaack, M.; Göbel, T. Investigations Concerning the Reaction Silica/Organosilane and Organosilane/Polymer. Part 1: Reaction Mechanism and Reaction Model for Silica/Organosilane. *Kautsch. Gummi Kunstst.* **1997**, *50*, 881−889.
(28) Okel, T. A.; Waddell, W. H. Silica Properties/Rubber Performance Correlation. Carbon Black-Filled Rubber Compounds. *Rubber Chem. Technol.* **1994**, *67* (2), 217−236.
(29) Wang, M.-J. Effect of Polymer-Filler and Filler-Filler Interactions on Dynamic Properties of Filled Vulcanizates. *Rubber Chem. Technol.* **1998**, *71* (3), 520−589.
(30) Sekar, P.; Noordermeer, J. W. M.; Anyszka, R.; Gojzewski, H.; Podschun, J.; Blume, A. Hydrothermally Treated Lignin as a Sustainable Biobased Filler for Rubber Compounds. *ACS Appl. Polym. Mater.* **2023**, *5*, 2501.
(31) Sekar, P. Design of a Bio-Based Filler System for Tire Treads, PDEng Thesis University of Twente: The Netherlands, 2018.
(32) Balakshin, M. Y.; Capanema, E.; Santos, R.; Chang, H.-M.; Jameel, H. Structural Analysis of Hardwood Native Lignins by Quantitative 13C NMR Spectroscopy. *Holzforschung* **2016**, *70*, 95.
(33) Zhu, X.; Zhang, D.; Lu, R.; Lu, F. Formation of Lignin Alkyl-O-Alkyl Ether Structures via 1,6-Addition of Aliphatic Alcohols to β-O-4-Aryl Ether Quinone Methides. *Org. Biomol. Chem.* **2023**, *21* (28), 5840−5854.
(34) Fulmer, G. R.; Miller, A. J. M.; Sherden, N. H.; Gottlieb, H. E.; Nudelman, A.; Stoltz, B. M.; Bercaw, J. E.; Goldberg, K. I. NMR Chemical Shifts of Trace Impurities: Common Laboratory Solvents, Organics, and Gases in Deuterated Solvents Relevant to the Organometallic Chemist. *Organometallics* **2010**, *29* (9), 2176−2179.
(35) Lee, W.; Tonelli, M.; Markley, J. L. NMRFAM-SPARKY: Enhanced Software for Biomolecular NMR Spectroscopy. *Bioinformatics* **2015**, *31* (8), 1325−1327.
(36) *Spectral Database for Organic Compounds*. SDBSWeb. https://sdbs.db.aist.go.jp (National Institute of Advanced Industrial Science and Technology) (accessed 2022−09−01).
(37) Wu, D. H.; Chen, A. D.; Johnson, C. S. An Improved Diffusion-Ordered Spectroscopy Experiment Incorporating Bipolar-Gradient Pulses. *J. Magn. Reson. A* **1995**, *115* (2), 260−264.
(38) Li, W.; Chung, H.; Daeffler, C.; Johnson, J. A.; Grubbs, R. H. Application of 1H DOSY for Facile Measurement of Polymer Molecular Weights. *Macromolecules* **2012**, *45* (24), 9595−9603.
(39) Baccile, N.; Laurent, G.; Babonneau, F.; Fayon, F.; Titirici, M.-M.; Antonietti, M. Structural Characterization of Hydrothermal Carbon Spheres by Advanced Solid-State MAS 13C NMR Investigations. *J. Phys. Chem. C* **2009**, *113* (22), 9644−9654.
(40) Calucci, L.; Rasse, D. P.; Forte, C. Solid-State Nuclear Magnetic Resonance Characterization of Chars Obtained from Hydrothermal Carbonization of Corncob and Miscanthus. *Energy Fuels* **2013**, *27* (1), 303−309.
(41) Salon, M. B.; Gerbaud, G.; Abdelmouleh, M.; Bruzzese, C.; Boufi, S.; Belgacem, M. N. Studies of Interactions between Silane Coupling Agents and Cellulose Fibers with Liquid and Solid-State NMR. *Magn. Reson. Chem.* **2007**, *45* (6), 473−483.
(42) Brochier Salon, M.-C.; Belgacem, M. N. Hydrolysis-Condensation Kinetics of Different Silane Coupling Agents. *Phosphorus, Sulfur Silicon Relat. Elem.* **2011**, *186* (2), 240−254.

(43) Hemmingson, J. A.; Leary, G. The Self-Condensation Reactions of the Lignin Model Compounds, Vanillyl and Veratryl Alcohol. *Aust. J. Chem.* **1980**, *33* (4), 917−925.
(44) Shevchenko, S. M.; Apushkinsky, A. G.; Zarubin, M. Y. On Regioselectivity of the Reaction of P-Quinone Methides with p-Hydroxybenzyl Alcohols. *Wood Sci. Technol.* **1992**, *26* (5), 383−392.
(45) Komatsu, T.; Yokoyama, T. Revisiting the Condensation Reaction of Lignin in Alkaline Pulping with Quantitativity Part I: The Simplest Condensation between Vanillyl Alcohol and Creosol under Soda Cooking Conditions. *J. Wood Sci.* **2021**, *67* (1), 45−57.
(46) Leary, G. J. Quinone Methides and the Structure of Lignin. *Wood Sci. Technol.* **1980**, *14* (1), 21−34.
(47) Coles, B. Effects of Modifying Structure on Electrophilic Reactions with Biological Nucleophiles. *Drug Metab. Rev.* **1984**, *15* (7), 1307−1334.
(48) Bolton, J. L.; Turnipseed, S. B.; Thompson, J. A. Influence of Quinone Methide Reactivity on the Alkylation of Thiol and Amino Groups in Proteins: Studies Utilizing Amino Acid and Peptide Models. *Chem. Biol. Interact.* **1997**, *107* (3), 185−200.
(49) Toteva, M. M.; Richard, J. P. The Generation and Reactions of Quinone Methides. *Adv. Phys. Org. Chem.* **2011**, *45*, 39−91.
(50) Ferrandin-Schoffel, N.; Haouas, M.; Martineau-Corcos, C.; Fichet, O.; Dupont, A.-L. Modeling the Reactivity of Aged Paper with Aminoalkylalkoxysilanes as Strengthening and Deacidification Agents. *ACS Appl. Polym. Mater.* **2020**, *2* (5), 1943−1953.
(51) Arkles, B.; Steinmetz, J.; Zazyczny, J.; Mehta, P. Factors Contributing to the Stability of Alkoxysilanes in Aqueous Solution. *J. Adhes. Sci. Technol.* **1992**, *6*, 193−206.
(52) Pearson, R. G. Hard and Soft Acids and Bases—the Evolution of a Chemical Concept. *Coord. Chem. Rev.* **1990**, *100*, 403−425.
(53) LoPachin, R. M.; Geohagen, B. C.; Nordstroem, L. U. Mechanisms of Soft and Hard Electrophile Toxicities. *Toxicology* **2019**, *418*, 62−69.
(54) Brinker, C. J. Hydrolysis and Condensation of Silicates: Effects on Structure. *J. Non-Cryst. Solids* **1988**, *100* (1−3), 31−50.

https://doi.org/10.1021/acssuschemeng.3c03497
ACS Sustainable Chem. Eng. 2023, 11, 16882−16892